LBNL-49018
DA-438

Accepted for publication in a special issue of Energy and Buildings.

A METHOD FOR SIMULATING THE PERFORMANCE OF PHOTOSENSOR-BASED LIGHTING CONTROLS

Charles Ehrlich, Konstantinos Papamichael, Judy Lai, and Kenneth Revzan
Building Technologies Department
Environmental Energy Technologies Division
Ernest Orlando Lawrence Berkeley National Laboratory
1 Cyclotron Road,
Berkeley, CA 94720 USA

October 2001

This research effort was funded by the Pacific Gas & Electric Company (PG&E) through the California Institute for Energy Efficiency (CIEE), a research unit of the University of California. Publication of research results does not imply CIEE endorsement of or agreement with these findings, nor does it indicate the endorsement or agreement of any CIEE sponsor. Pacific Gas & Electric Company's funding is provided by California utility customers under the auspices of the California Public Utilities Commission. This work was also supported by the Assistant Secretary for Energy Efficiency and Renewable Energy, Office of Building Technology, State and Community Programs, Office of Building Research and Standards of the U.S. Department of Energy under Contract No. DE-AC03-76SF00098.

A METHOD FOR SIMULATING THE PERFORMANCE OF PHOTOSENSOR-BASED LIGHTING CONTROLS

Charles Ehrlich[1], Konstantinos Papamichael, Judy Lai, and Kenneth Revzan
Building Technologies Department
Environmental Energy Technologies Division
Ernest Orlando Lawrence Berkeley National Laboratory
1 Cyclotron Road, Berkeley, CA 94720 USA

Abstract

The unreliability of photosensor-based lighting controls continues to be a significant market barrier that prevents widespread acceptance of daylight dimming controls in commercial buildings. Energy savings from the use of daylighting in commercial buildings is best realized through the installation of reliable photoelectric lighting controls that dim electric lights when sufficient daylight is available to provide adequate background and/or task illumination. In prior work, the authors discussed the limitations of current simulation approaches and presented a robust method to simulate the performance of photosensor-based controls using an enhanced version of the Radiance lighting simulation package. The method is based on the concept of multiplying two fisheye images: one generated from the angular sensitivity of the photosensor and the other from a 180- or 360-degree fisheye image of the space as "seen" by the photosensor. This paper includes a description of the method, its validation and possible applications for designing, placing, calibrating and commissioning photosensor-based lighting controls.

Introduction

Controlling the output of electric lights using photosensor-based lighting controls can result in significant energy savings resulting from daylighting while preserving or improving occupant comfort and productivity [1]. However, use of such controls has been unreliable in large part because of the significant effort required to properly place and calibrate the photosensor system. Proper commissioning involves calibrating the system under many different daylighting conditions that may occur in the controlled space. Multiple visits to the building after construction is complete are often cost prohibitive. Moreover, there is a variety of photosensors to choose from and no easy way to predict and compare performance among them.

Predicting the performance of the electric lighting control system and its effects on energy use and other performance characteristics requires accurate computation of daylighting and electric lighting levels and reliable simulation of the photosensor's behavior in response to the variable lighting conditions in which it is installed [2]. The unreliability of photosensor-based lighting control systems continues to be a significant market barrier preventing widespread acceptance of daylight dimming controls in commercial buildings. This paper is about a new method that allows accurate simulation of photosensor-based controls that can be used to assist in the design, selection, placement, and commissioning of photosensor-based daylight dimming systems. The method can be used to design photosensors for specific building applications (for example, small offices with north-facing vertical glazing) and promotes the successful installation and operation of photosensor-based controls by minimizing the need for difficult and expensive on-site commissioning.

This paper describes a simulation method that is based on consideration of the geometric and material conditions of the space and the angular sensitivity, color correction filter, and placement of the photosensor. The paper also includes a description of the method's implementation using an expanded version of the Radiance lighting simulation software, as well as results of a validation exercise in which the method is shown to accurately predict the photosensor signal strength of a photosensor-controlled lighting system installed at the Oakland Federal Building [3]. The paper describes how the method can be used in the design of photosensor-based controls as well as in their installation, calibration, and operation. Furthermore, the method can be used to pre-calibrate a specific proposed photosensor-controlled lighting system in a virtual office space to determine how effectively the system will operate.

[1] Now with the Heschong Mahone Group, 11626 Fair Oaks Blvd. #302, Fair Oaks, California, 95628 USA.

Background

Typical photosensor-based electric lighting control systems for commercial offices include a photosensor strategically mounted either on the ceiling or under the luminaire close to the daylight aperture (see **Figure 1**). A typical photosensor is a silicon photodiode equipped with a diffuser that integrates the luminance of the surrounding surfaces. Some photosensors have a hemispherical view of the room whereas others have a view that extends beyond the hemisphere.

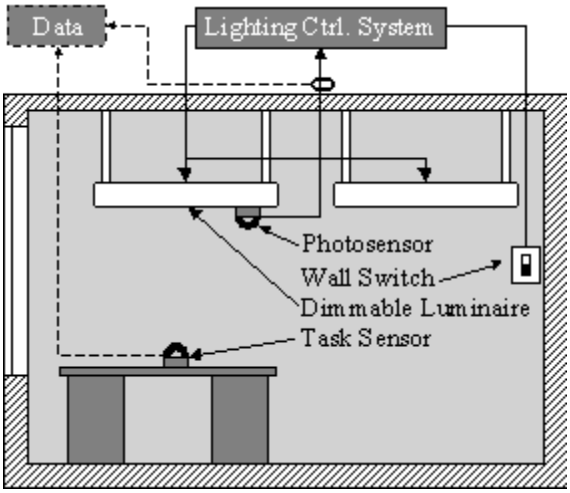

Figure 1. Schematic diagram of a typical installation of photosensor-based controls in a commercial office space. Lines indicate power or data connections between components. Dashed arrows indicate connections and components needed only for collecting performance data.

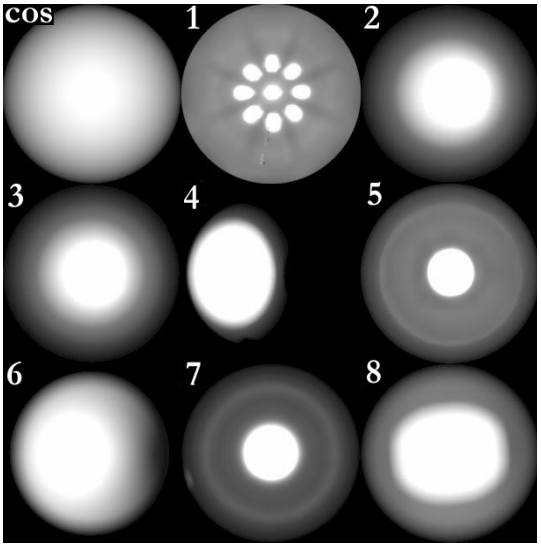

Figure 2. An ideal cosine spatial sensitivity distribution plus the eight photosensor distributions of Bierman and Conway, shown here as fisheye images.

Different photosensors models vary significantly in their angular and spectral sensitivity to light among different sensors (see **Figure 2**) with some sensors being highly sensitive within a very narrow angle, others having a non-symmetrical sensitivity. Silicon photodiodes are sensitive to a different band of the electromagnetic spectrum than the human eye; their sensitivity extends into the UV and IR ranges. Therefore, photosensors are usually equipped with a color correction filter to approximate the human eye's response to light. A variety of simple electrical control circuits adjust the photosensor output signal voltage [1] based on the photosensor's signal.

The photosensor circuitry is connected to the lighting control system, which dims the electric lights when adequate daylight is available, and increases electric lighting when daylight availability drops, in order to maintain adequate workplane illuminance levels. Problems with the design, simulation, and calibration of such systems arise when it is assumed that the photosensor signal is a reliable measure of workplane illuminance. In fact, the photosensor response is a function of the luminance distribution of all surfaces seen by the sensor.

Photosensor controls often do not work as expected and, as a result, room occupants often do not accept them [4] [5]. One reason why they do not work is because the designer does not have a comprehensive understanding of their actual performance during the design phase of the project. Attempts to repair an improper installation usually fail because important factors such as the placement and selection of the photosensor device are not feasible to change.

Research performed by Bierman and Conway [6] demonstrates that different photosensor models have different acceptance angles and widely varying spatial and spectral sensitivities. The color-correction filter used with most sensors does not adequately approximate the photometric curve. Photosensor behavior can vary widely depending upon the sensor's placement in the room, the room surface reflectance, the placement of furniture, and the sensor's view of brightly lit exterior surfaces.

The Bierman and Conway study provides the data necessary to improve the accuracy of simulations of the actual performance of photosensors. The varied angular responses of the eight photosensors considered in their study are shown in **Figure 2** along with a theoretical cosine-corrected photosensor distribution. These data are provided in a two-dimensional file containing the relative sensor signal strength at each altitude and azimuth orientation.

The spectral response of these photosensors also varies. **Figure 3** shows three spectral curves that represent the eight photosensors of the Bierman and Conway study plotted against the Commission International de l'Eclairage (CIE) 1924 V-lambda photometric curve. The three representative calibration filters do not accurately estimate the V-lambda curve. Most important, the error varies significantly (depending upon photosensor model) for different sources (see **Figure 4**), which is difficult to account for in the lighting control algorithm. This means that some photosensors will respond differently to different combinations of daylight and electric light.

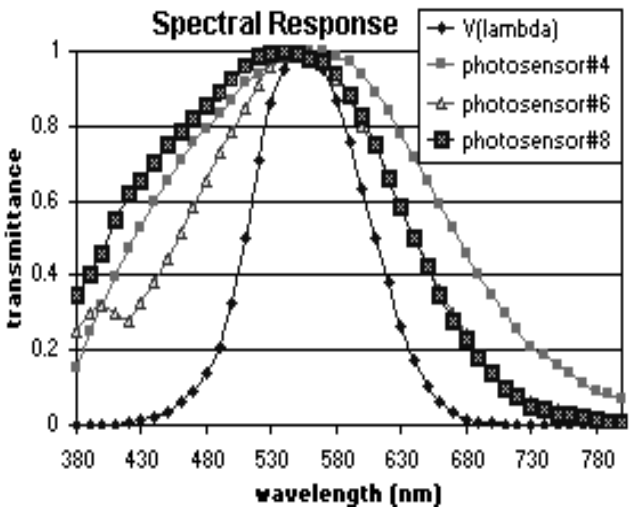

Figure 3. Three representative photometric correction filters and the CIE 1924 V-lambda photometric curve, an ideal color correction used to convert spectral radiance to illuminance.

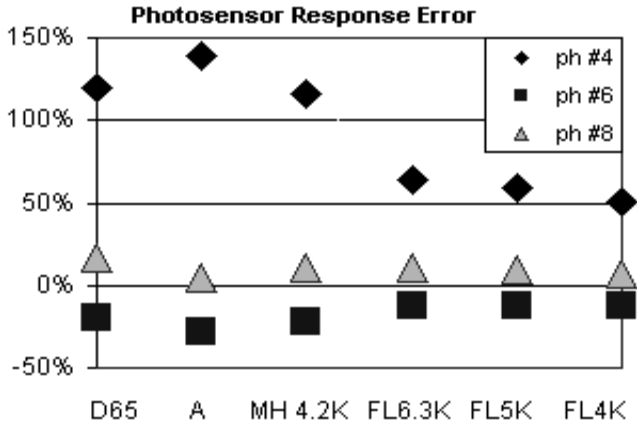

Figure 4. Relative error of three representative spectral curves illuminated by daylight (D65), incandescent (A), 4200K Metal Halide (MH 4.2K), 6300K fluorescent (FL6.3K), 5000K fluorescent (FL5K), and 4000K fluorescent (FL4K).

Simulation Method

The new method computes photosensor performance based on the notion that the view of a photosensor and its angular sensitivity data can be represented by fisheye images (see **Figure 2**). The fisheye projection maps points that are 180 degrees from the nadir to a circle equidistant from the center of the image. Where the photosensor is more sensitive to light, the fisheye image will be whiter (corresponding to larger values) and where it is less sensitive, it will be blacker (corresponding to smaller values). Furthermore, the particular view of the room as "seen" by the photosensor can also be represented by a color, fisheye image (**Figure 5**). The predicted photosensor signal is idealized as the pixel-by-pixel multiplication of these two fisheye images, one generated from the angular acceptance curve of the control photosensor and the other from a 180- or 360-degree fisheye *Radiance* [7] simulation of the space as "seen" by the photosensor. The sum of the pixel values of the new fisheye image, adjusted by the photosensor's spectral response, corresponds to the signal of the photosensor and can be converted to the actual output voltage by multiplication with an appropriate scaling factor. This scaling factor represents the internal gains of the circuitry of the photosensor. In the absence of this information from the manufacturer, the scaling factor can be determined with measurements of the photosensor response voltage under controlled conditions.

The method requires accurate modeling of the scene in three dimensions, including interior as well as exterior surface optical properties. The image-generation process must accurately account for the interaction of light with all surfaces and materials and must accurately account for the luminance of the sky dome and solar disk. Although a variety of simulation programs offer many of these capabilities, only *Radiance* offers an accurate representation of the sky-dome luminance (when viewed directly) and can

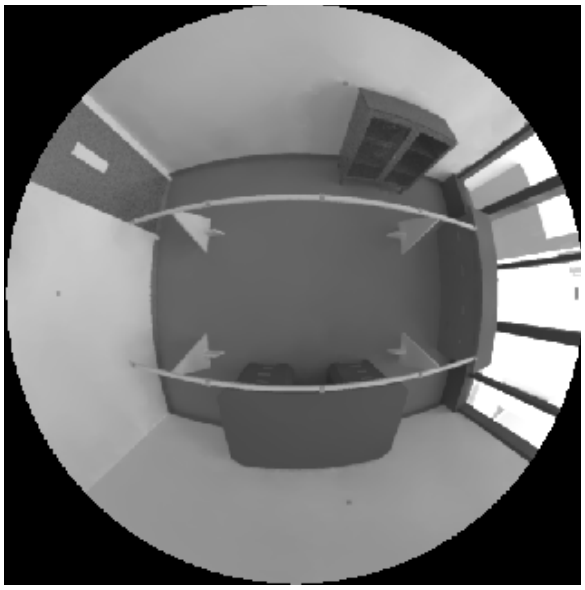

Figure 5. This 180-degree fisheye image shows the model of the room used for validation of the simulation method from the perspective of a photosensor mounted under the pendant luminaire. Notice the windows on the right side showing brightly illuminated exterior surfaces.

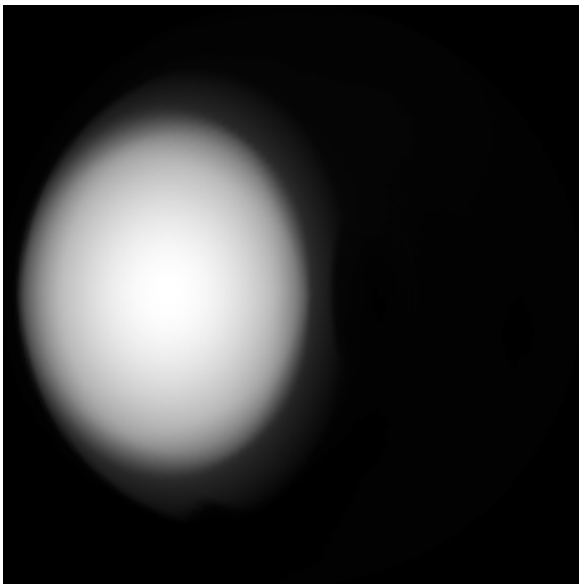

Figure 6. An example photosensor sensitivity fisheye image showing a strong lateral bias. This type of photosensor is often used next to windows to reduce the effect of bright exterior surfaces on the photosensor signal.

generate fisheye images. *Radiance's* daylighting prediction accuracy has been extensively validated by independent researchers [8] [9].

An overview of the use of the simulation method is described below. For a more detailed discussion, see the authors' previous work [10].

The first step is to generate a fisheye image that represents the angular sensitivity of the photosensor. A new Radiance module called **`mksens`** has been developed to convert photosensor data into an RGB image. This image can then be viewed to determine the spatial orientation of the photosensor (**Figure 2**). This new module allows the specification of thedesired resolution of the output image and is used through the following syntax:

```
mksens [-r resolution] "sensitivity
file" > "radiance image"
```

where resolution refers to the resolution of the output image in pixels.

Figure 6 shows the sensitivity image of a photosensor with a strong lateral bias. If this sensor's intended use will direct its more sensitive side toward the back of the room, then the appropriate rotation of the data can be determined. The photosensor in **Figure 6** is appropriately oriented for placement in the room shown in **Figure 5**, so no rotation of the spatial data is necessary sensitivity.

The second step in the simulation process is to develop a model of the scene geometry and surface optical properties. The model may be of any degree of complexity, and it should include furniture and appropriate glazing specifications. Achromatic material specifications can be used if strong colors are not likely to be present in the room. However, this may introduce some error because of the photometric calibration of the photosensors. Extra care should be taken to model nearby exterior geometry, such as the ground surface or neighboring buildings, because the brightness of these surfaces can be hundreds of times greater than the brightness of the interior surfaces. Even a small fraction of a brightly-lit exterior surface can have a significant effect on the signal generated by the photosensor.

The third step in the simulation method is to compute a fisheye image of the space from the location and in the view direction of the photosensor, as shown in **Figure 5**. If the photosensor acceptance angle extends beyond a hemisphere, then a 360-degree fisheye must be rendered.

The fourth step is to convert the photometric correction filter spectral data file into a *Radiance* red, green, blue approximation. The Radiance RGB color specification format represents a three-point sampling of the visible spectrum. The spectral sensitivity data must be converted into the RGB format to allow for proper consideration of the varying spectral selectivity of different photosensors. This conversion process is described in detail in *Rendering with Radiance* [7].

The final step is to compute the product of the photosensor sensitivity and room fisheye images using a newly developed software module called **psens**. This module multiplies the image pixel values, sensitivity factor, and solid angle weight to give an integrated signal response. The sum of the interpolated pixel values is multiplied by the color correction factor specified as a red, green, blue triplet (determined in the previous step) to provide the final result, i.e., the predicted signal of the photosensor. Equation 1 explains the relationship between total photosensor response and the input parameters.

$$R = \sum \left[B_R S_R(\vartheta,\varphi) P_R(\vartheta,\varphi) B_G S_G(\vartheta,\varphi) P_G(\vartheta,\varphi) + B_B S_B(\vartheta,\varphi) P_B(\vartheta,\varphi) \right] \cdot \Omega(\vartheta,\varphi) \qquad (1)$$

where B is brightness coefficient, S is photosensor sensitivity, P is pixel value, and Ω is the solid angle subtended by the square surrounding the pixel. The suffix indicated the color and each pixel is represented by its spherical coordinates, θ and Φ.

The command syntax to use **psens** in this last step are:

```
psens -s "sensitivity file" [-r rotation] [-R redSens -G grnSens -B
bluSens] "radiance image"
```

where rotation is the number of degrees to rotate the spatial sensitivity data to align the sensor with the desired orientation relative to the room fisheye image. The output results show the following:

```
Total solid angle: 7.45591
Total sensitivity: 2.20607
Response: 48.0008
```

where the total solid angle is the spatial extent of the sensitivity data (in steradians), total sensitivity is the sum of the sensitivity factors as found in the input file, and response is the predicted photosensor signal strength.

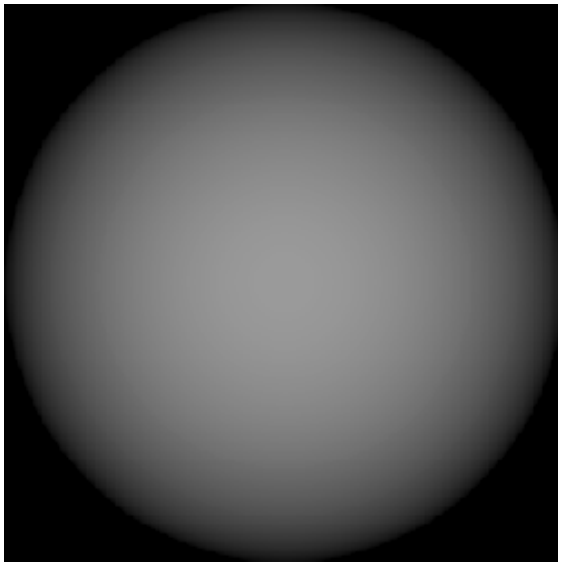

Figure 7. This image shows the ideal, cosine-corrected photosensor sensitivity distribution. The sum of the pixel brightness of this image is 1.0; it was used to validate the angular summation code.

Validation

The authors validated their simulation method using hypothetical data to verify the code and actual data collected from an office installation at the Oakland Federal Building. Code validation involved comparing the output from **psens** with a known data set to verify that the pixel area weighting assumptions provide accurate results. A cosine distribution data file was computed and used to verify that **psens** would compute a value of 1.0. The image created from this dataset represents a perfect cosine-corrected photosensor (see **Figure 7**). If the input image is of sufficient resolution (at least 200 by 200 pixels), the pixel area weighting factors do not show appreciable error.

Validation with experimental data was based on data from the Oakland Federal Building (OFB). The OFB testbed, located in Oakland, California (37º4' N, 112º1' W), is a pair of furnished office spaces outfitted with photosensor-controlled lighting systems, task photosensors, and data collection equipment (**Figures 8 and 9**). The collected data include interior workplane illuminance and photosensor signal strength taken every five minutes. The data were analyzed to find three spring days on which exterior illuminance remained fairly

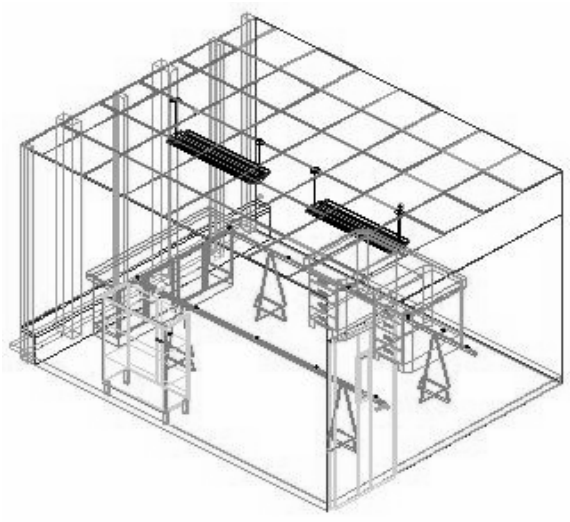

Figure 8. Wire-line image showing AutoCADTM 3-D model of the Oakland Federal Building office used for experimental validation of the simulation method.

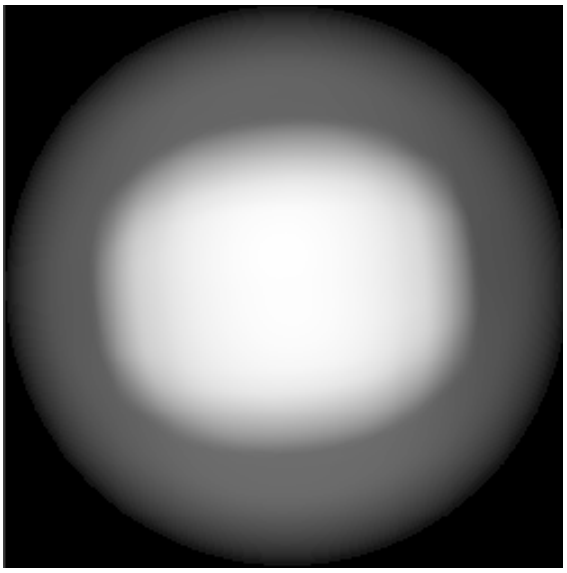

Figure 9. Spatial distribution fisheye image of the photosensor used in the Oakland Federal Building .

constant, indicating that there was no cloud cover, and during which the lighting system was completely dimmed (0.0 percent) because daylighting was sufficient. Clear days were selected to avoid introducing arbitrary error into the validation exercise with the complexities of the interaction of direct beam sunlight with fenestration apertures. March 18, 3:00 PM, April 16, 3:00 PM and May 17, 3:00 PM were selected (see **Table 1**). Photosensor signal strength in volts and workplane illuminance in lux were recovered from the data set and averaged from these three days when the lights were off. In addition, we collected data from a nighttime condition with lights at 100 percent power. We computed lux per volt for each of these days and then computed the average of these three days to minimize error resulting from changing sky conditions.

Table 1. Sensor Voltage and Workplane Illuminance for Three Daytime and One Nighttime Measurement at the Oakland Federal Building

Daylight Only				
Date	**Time**	**Volts**	**Lux**	**Lux/Volt**
March 18	3:00 PM	2.61	645	247
April 16	3:00 PM	2.95	733	248
May 17	3:00 PM	3.36	797	237
			Avg.	**244**
Electric Light Only				
		1.00	585	585
Average task-sensor ratio for daylight				244
Task-sensor ratio for electric light				585
Task-sensor electric/daylight ratio				**2.39**

The ratio of task illuminance to photosensor signal voltage (task-sensor ratio) was selected as the basic measure of photosensor performance [11]. The validation exercise compared the measured and simulated values for the task-sensor ratio for daylight only and electric light only conditions. A Radiance simulation of these same conditions was computed using the CIE clear sky model (**gensky**). The resulting fisheye images were processed with the **psens** program. We also attempted to validate the absolute light levels by computing fisheye images at the workplane and at the photosensor multiplied by the ideal cosine sensitivity distribution to compare the task and photosensor illuminance levels in *Radiance* with the nighttime measured conditions. As shown in **Table 2**, agreement for the electric lighting condition task-sensor ratio is quite strong with error of only 1.4 percent. The daylight condition also shows good agreement in the task-sensor ratio; this agreement could probably be improved if the Perez sky model [12] were used instead.

Table 2. Validation Results

Description	Measured	Simulated	Error %
Daylighting task-sensor ratio	2.39	2.55	+6.7
Electric lighting task illuminance	485.0 lux	453.64 lux	–6.5
Electric lighting sensor illuminance	94.0 lux	89.02 lux	–5.3
Electric lighting task-sensor ratio	5.16	5.09	–1.4

Applications

The availability of ray-tracing-based lighting simulation software (e.g., *Radiance*) and measured data for the angular and spectral sensitivity of photosensors makes it possible to effectively simulate the operation of photosensor-based electric lighting controls. The method described in this paper computes the signal of a photosensor by multiplying two fisheye images, one representing the angular sensitivity of the photo sensor and the other representing the scene luminance as seen by the sensor, and summing the resulting pixel values.

The method presented above is useful for manufacturers of photosensor controls to help with product design and to optimize control algorithms. It is also useful for the design of specific applications of photosensor-based controls as well as for their calibration, by allowing virtual operation in a CAD model of the space for multiple days and times during a year. The method can handle arbitrarily complex geometric configurations and complex fenestration systems, such as those incorporating Venetian blinds. The method provides immediate feedback in the form of a fisheye image of the photosensor angular sensitivity orientation. It makes few assumptions, is highly accurate, and considers the effect of surface reflectance, geometric configurations, exterior shading, photosensor placement, and photometric calibration filters.

In the absence of a comprehensive CAD-integration solution, the **mksens** and **psens** programs are valuable tools on their own. A manufacturer or product designer can use the *Desktop Radiance* software to develop a set of static prototypical spaces with varying layouts and orientations. The simulation models and the appropriate sensor parameters can then be fed into *Radiance for Windows* for generating a set of parametric simulations for a random sampling of typical sky and weather conditions. The workplane illuminance and predicted photosensor response are thus computed. The output of these parametric simulations will provide a scatter plot of the simulated workplane illuminance versus the predicted photosensor response. A simple graphing tool can display this scatter plot and find a closest fit line. This line represents the ideal performance of the photosensor control algorithm. Alternative control strategies can also be represented on this scatter plot. For example, if the

control strategy is to maximize energy savings while allowing the workplane illuminance to drop below optimum a certain percentage of the time, a line can be fit toward the bottom of the scatter plot. Conversely, if the control strategy must maintain strict adherence to the minimum workplane illuminance, then a line can be fit to the upper bounds of the scatter plot.

This graphing and plotting tool can be further refined by plotting the actual response of the photosensor control circuitry with control "joints" tied to input variables that represent the adjustments of the actual physical device. Then, the parametric simulations can be re-computed using the actual photosensor response curve to estimate the annual energy savings. Just as the product designer can use this method to predict the energy savings of a future product, so too can a lighting designer predict energy savings from the installation of a particular photosensor into a particular building location.

While seemingly trivial in its presentation, the **`mksens`** program is a key component of this method because it allows the designer to visualize the hemispherical sensitivity of the photosensor. As shown above, some photosensors have asymmetrical distributions. This feature of the sensor can be used to the designer's advantage when it is oriented either toward or away from the primary window aperture, according to the control strategy the designer selects (see **Figure 10**).

This method is limited by the lack of widely available angular sensitivity information on specific photosensor. Manufactures do not yet supply this information their products partly due to a lack of demand and partly because no standard exists for the encoding and transfer of photosensor information. It is hoped that publications such as *Specifier Reports* [13] will include these data in the future and that the appropriate committees of the Illuminating Engineering Society will find the time to specify an appropriate file format. The system has been validated only in a commercial office setting with vertical glazing, but it is applicable to other building types and glazing systems.

Future plans are to include the new method in *Desktop Radiance* [14], a Windows™ version of *Radiance* that has links to *AutoCAD*, which will make the program easier and faster to use. Integration of the new method in *Desktop Radiance* will allow architects and lighting designers to more readily evaluate alternative lighting control designs within a familiar CAD environment.

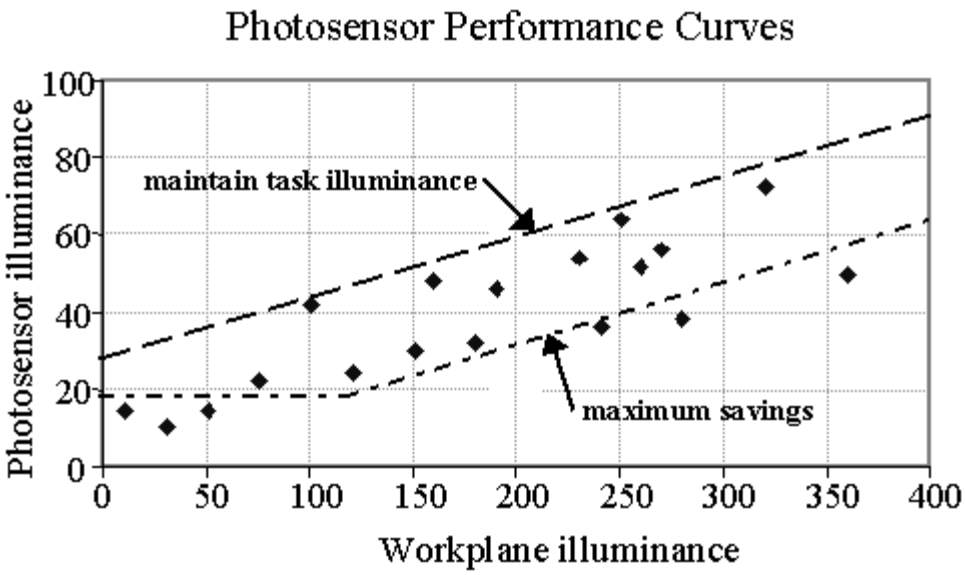

Figure 10. Scatter plot of simulated workplane illuminance versus photosensor-predicted workplane illuminance. Lower line shows control strategy to maximize energy savings while the upper line shows a strategy to maintain task illuminance levels in all cases.

Acknowledgments

This research effort was funded by the Pacific Gas & Electric Company (PG&E) through the California Institute for Energy Efficiency (CIEE), a research unit of the University of California. Publication of research results does not imply CIEE endorsement of or agreement with these findings, nor does it indicate the endorsement or agreement of any CIEE sponsor. Pacific Gas & Electric Company's funding is provided by California utility customers under the auspices of the California Public Utilities Commission. This work was also supported by the Assistant Secretary for Energy Efficiency and Renewable Energy, Office of Building Technology, State and Community Programs, Office of Building Research and Standards of the U.S. Department of Energy under Contract No. DE-AC03-76SF00098. The authors give special thanks to Richard Mistrick and Francis Rubinstein for their valuable feedback during the refinement of the simulation technique, to Pacific Gas and Electric for providing the photosensor acceptance data, to Eleanor Lee for providing the Oakland Federal Building data, and to Dr. Guedi Capeluto of the Technion IIT for his helpful comments and review of the draft paper.

References

[1] Rubinstein, F. 1984. Photoelectric Control of Equi-ilumination Lighting Systems. *Energy and Buildings* Vol.6(1084): 141-150.

[2] Mistrick, R. and Thongtipaya, J. 1997. "Analysis of Daylight Photocell Placement and View in a Small Office" *Journal of the IESNA* Vol. 26(no. 2):150-160.

[3] Lee, Eleanor, DiBartolomeo, D., Selkowitz, S. 1998. "Thermal and daylighting performance of an automated venetian blind and lighting system in a full-scale private office." *Energy and Buildings*. August: 47-63.

[4] Love, J. 1995. "Field Performance of Daylighting Systems with Photoelectric Controls, " Presented at *3rd European Conference on Energy-Efficient Lighting*, Newcastle-upon-Tyne, UK.

[5] Mistrick, R., Chen, C., Bierman, A., and Felts, D. 2000. "A Comparison of Photosensor-Controlled Electronic Dimming Systems in a Small Office." *Journal of the IESNA* Vol. 28(no. 1): 59-73.

[6] Bierman, A and Conway, K. 2000. Characterizing Daylight Photosensor System Performance to Help Overcome Market Barriers. *Journal of the IESNA* Vol. 29(no. 1): 101-115.

[7] Ward, G. and Shakespeare, R. 1999. *Rendering With Radiance.* Morgan Kaufman. San Francisco.

[8] Khodulev, A., Kopylov, E. 1996 Physically Accurate Lighting Simulation in Computer Graphics Software. Keldysh Institute of Applied Mathematics, Russian Academy of Sciences. Moscow State University. Moscow.

[9] Mardaljevic, J. 1995. Validation of a lighting simulation program under real sky conditions Lighting Res. Technology. 27(4) 181-188.

[10] Ehrlich, C., Papamichael, K., Lai, J., Revzan, K. 2001. Simulating the Operation of Photosensor-based Lighting Controls. *Building Simulation 2001*. IBPSA.

[11] Rubinstein, F., Ward, G., and Verderber, R. 1989. "Improving the Performance of Photo-Electrically Controlled Lighting Systems," *Journal of the IESNA*, Vol. 18(no. 1): 70-94.

[12] Perez, R., R. Seals, and R. J. Michalsky. 1993. All-Weather Model for Sky Luminance Distribution, Preliminary Configuration and Validation. Solar Energy, 50(3), 235-45.

[13] National Lighting Product Information Program. 1988. *Specifier Reports: Photosensors*. Vol. 6; no. 1, Troy, NY: Lighting Research Center, Rensselaer Polytechnic Institute.

[14] LBNL. 2000. The Desktop Radiance web site is: http://radsite.lbl.gov/deskrad